Optical Rabi Oscillations in a Quantum Dot Ensemble

Mamiko Kujiraoka[1,2], Junko Ishi-Hayase[1,3,4*], Kouichi Akahane[1],
Naokatsu Yamamoto[1], Kazuhiro Ema[2], and Masahide Sasaki[1†]

[1]*National Institute of Information and Communications Technology (NICT), Koganei, Tokyo 184-8795, Japan*
[2]*Department of Physics, Sophia University, Chiyoda, Tokyo 102-8554, Japan*
[3]*The Center for Frontier Science and Engineering, The University of Electro-Communications, Chofu, Tokyo 182-8585, Japan*
[4]*PRESTO, Japan Science and Technology Agency (JST), Kawaguchi, Saitama 332-0012, Japan*

Received July 4, 2010; accepted July 25, 2010; published online August 20, 2010

We have investigated Rabi oscillations of exciton polarization in a self-assembled InAs quantum dot ensemble. The four-wave mixing signals measured as a function of the average of the pulse area showed the large in-plane anisotropy and nonharmonic oscillations. The experimental results can be well reproduced by a two-level model calculation including three types of inhomogeneities without any fitting parameter. The large anisotropy can be well explained by the anisotropic dipole moments. We also find that the nonharmonic behaviors partly originate from the polarization interference.

DOI: 10.1143/APEX.3.092801

Optical Rabi oscillations (ROs) play a central role in a variety of applications involving a discrete system where the coherent light-matter interactions are optically controlled.[1–9)] Exciton ground-states in semiconductor quantum dots (QDs) have been attractive solid-state candidates for implementing those applications because they exhibit atomlike discrete energy levels, large transition dipole moments, and long dephasing time. Excitonic ROs in single QDs have been reliably established by the observation of sinusoidal oscillations of the exciton population[1–6)] (the vertical component of the Bloch vector) or exciton polarization[8)] (the horizontal component) as a function of the pulse area of the excitation pulse. In the case of QD ensembles, a nontrivial analysis is necessary to confirm the observation of ROs since various types of ensemble effects may cause huge deviations of macroscopic behavior of excitonic ROs from the ideal ROs in a two-level system. Although the coherent light-matter interactions in a QD ensemble are important issues for many applications, so far only two groups have reported the observation of excitonic ROs in it.[7,9)] In quantum islands in a GaAs single quantum well where excitons were weakly confined, it was found that the prominent exciton–exciton interactions complicated the RO behaviors.[9)] Even using self-assembled InGaAs QDs where the interdot interactions were significantly suppressed due to the strong confinement energy, the dot-to-dot variation (the inhomogeneity) of the transition dipole moment strongly affected the ROs damping in the exciton population.[7)] On the other hand, a quantitative study of inhomogeneous effects on exciton polarization ROs has never been performed in any previous studies. Recently, our group pointed out that the effects of the nonuniform electric field on the ensemble-averaged ROs are quite different in the exciton population and in the exciton polarization.[10)] However, a thorough analysis considering all origins of the inhomogeneities remains an open issue.

In this letter, we investigate the exciton polarization ROs in a self-assembled InAs QD ensemble including anisotropic properties. The ensemble average of the inhomogeneously-distributed exciton polarization was measured using polarization-dependent four-wave mixing (FWM) techniques and analyzed by a calculation considering three types of inhomogeneities without any fitting parameter. We found that the large anisotropies of the oscillation amplitude and period are attributed to the anisotropic dipole moment. We also demonstrated that the nonharmonic nature of the observed ROs originates from polarization interference.

The sample was grown by molecular beam epitaxy on an InP(311)B substrate; it contained 150 layers of InAs self-assembled QDs embedded in 60-nm-thick $In_{0.52}Ga_{0.1}$-$Al_{0.38}As$ barrier spacers.[11)] The average-lateral size was estimated to be 51 nm in the $[\bar{2}33]$ direction and 39 nm in the $[01\bar{1}]$ direction, which was corresponding to the elongation ratio of 1.31. The average height was estimated to be 4 nm. The sample was fabricated using strain compensation to control the emission wavelength and to stack QD layers without degrading the crystalline quality. The total QD density exceeded $1 \times 10^{13}\,\mathrm{cm}^{-2}$ by stacking 150 QD layers. The high QD density is an advantage for enhancing weak FWM signals, which enables us to analyze ROs with a high degree of quantitative accuracy.[12)]

A pulse area dependence of the FWM signal intensities in the $2\boldsymbol{k}_2 - \boldsymbol{k}_1$ direction for two pulse excitations was measured to investigate the macroscopic behaviors of the exciton polarization ROs. In an ideal two-level system, the FWM signal amplitude, $\boldsymbol{S}_{\mathrm{FWM}}$ is proportional to $\mu \sin \Theta_{01} \sin^2(\Theta_{02}/2)$ for resonant excitation.[13)] Here, Θ_{0i} represents the area of the $\boldsymbol{k}_i$ pulse defined as time-integrated zero-detuning Rabi frequency, $\Omega_{0i} = \mu E_i(t, r)/\hbar$, where μ is the transition dipole moment and $E_i(t, r)$ is the electric field envelope. Therefore, a sinusoidal oscillation of the FWM intensity according to $\sin^2 \Theta_{01}$ is expected to be observed with increasing Θ_{01} while keeping the Θ_{02} constant. This oscillation is referred to as time-integrated ROs of excitonic polarization.

Excitation pulses were generated by a Ti:Sapphire-pumped optical parametric oscillator at a repetition rate of $\nu_{\mathrm{rep}} = 76\,\mathrm{MHz}$. The intensities of two excitation pulses showed Gaussian spatial distributions with the radii R at e^{-2} intensity of approximately 86 μm on the sample surface. The temporal profile of $E_i(t, r)$ can be expressed as $E_i(r)\,\mathrm{sech}(t/\tau_{\mathrm{sech}})$, $\tau_{\mathrm{sech}} = 0.55\,\mathrm{ps}$. The time delay between two excitation pulses was fixed at 20 ps. Both the pulse duration and the time delay are considerably shorter than

*Present address: Department of Applied Physics and Physico-Informatics, Keio University, Yokohama 223-8522, Japan.
†E-mail address: psasaki@nict.go.jp

the dephasing time of the ground-state excitons at low temperatures (>1 ns).[12] In addition, we confirmed that the dephasing time remained unchanged at all the excitation intensities of the $\boldsymbol{k}_1$ pulse used in the experiment. Therefore, any dephasing processes can be regarded as negligible in this study. The central wavelength of the excitation pulses was tuned to 1468 nm, which corresponds to the central wavelength of the exciton ground-state transitions. Two excitation pulses were collinearly polarized either in the $\boldsymbol{x} \parallel [01\bar{1}]$ or $\boldsymbol{y} \parallel [\bar{2}33]$ directions to selectively excite one of the ground states.[14] Due to the narrow bandwidth [a full width at half maximum (FWHM) = 1.7 meV] compared with the inhomogeneous broadening of the exciton ground-state transition energies (FWHM = 44 meV), approximately 10^8 QDs (only 4% of QDs in the beam spot) were resonantly excited. Since the bandwidth is narrower than the biexciton binding energy (≈3 meV), biexciton formation can be assumed to be of no significance for small pulse areas.

In this study, we determined the value of the pulse area independently of the FWM experiment. Since the electric field amplitude for each QD, $E(r,t)$, is different depending on the position in a QD ensemble, we define the average pulse area, $\bar{\Theta}_{0i}$ using the following relations, $\bar{\Theta}_{0i} = (\bar{\mu}\bar{E}_i/\hbar)\int \mathrm{sech}(t/\tau_{\mathrm{sech}})dt = \bar{\mu}\bar{E}_i\pi\tau_{\mathrm{sech}}/\hbar$ and $\bar{E}_i = (\bar{I}_i/cn\epsilon_0\tau_{\mathrm{sech}}\nu_{\mathrm{rep}})^{1/2}$ ($n = 3.51$ for InAs). $\bar{I}_i = \langle I_i\rangle/\pi R^2$ is the averaged excitation density calculated using the measured excitation power $\langle I_i\rangle$[15] and $\bar{\mu}$ is the ensemble average of the transition dipole moments. The values of $\bar{\mu}$ were estimated to be 58 ± 3 D for x-polarized excitons and 45 ± 3 D for y-polarized excitons from the radiative lifetimes measured by a pump-probe technique.[14] The ratio $\bar{\mu}^y/\bar{\mu}^x = 1.32$ is in quantitative agreement with the elongation ratio of the QD size mentioned above. This suggests that the large anisotropy of the $\bar{\mu}$ values is attributed to the asymmetric QD shape.[6,16] Due to the large anisotropy of $\bar{\mu}$, the excitation power $\langle I_i\rangle$ for $\bar{\Theta}_{0i} = \pi$ is anisotropic; $\langle I_i\rangle^{1/2}$ is 3.0 mW$^{1/2}$ for y-polarized excitons and 3.9 mW$^{1/2}$ for x-polarized excitons. In the experiment, $\bar{\Theta}_{01}$ was controlled by changing $\langle I_1\rangle^{1/2} \propto \bar{E}_1$ at constant τ_{sech}, while $\bar{\Theta}_{02}$ was fixed at $\simeq \pi$.

Figure 1 shows the FWM intensity measured as a function of $\langle I_1\rangle^{1/2}$ at 3 K for (a) y and (b) x polarizations. The period and amplitude of the observed oscillations show the large anisotropies with respect to the polarization directions of the excitation pulses. For both polarization directions, the FWM intensities approximately coincide with $\sin^2\bar{\Theta}_{01}$ for $\bar{\Theta}_{01} < 0.5\pi$ (shown by dashed lines in Fig. 1). For larger $\bar{\Theta}_{01}$, the discrepancy becomes prominent and the oscillations exhibit nonharmonic behaviors with increasing $\bar{\Theta}_{01}$: (1) the oscillation period is not constant, (2) the oscillation amplitudes strongly damp at $\bar{\Theta}_{01} < 2\pi$, (3) the FWM intensity increases again at $\bar{\Theta}_{01} > 2\pi$.

In order to analyze these nonharmonic behaviors, we performed theoretical calculations using the isolated two-level model considering three types of inhomogeneities: (1) spatial distribution of the excitation intensity, which leads to a position-dependent electric field amplitude[15] as $E_i(r) = \sqrt{2}\bar{E}_i\exp(-r^2/R^2)$, (2) inhomogeneous distribution of the transition dipole moment μ, and (3) inhomogeneous distribution of the detuning Δ between the excitation carrier frequency and the exciton ground-state transition frequency.

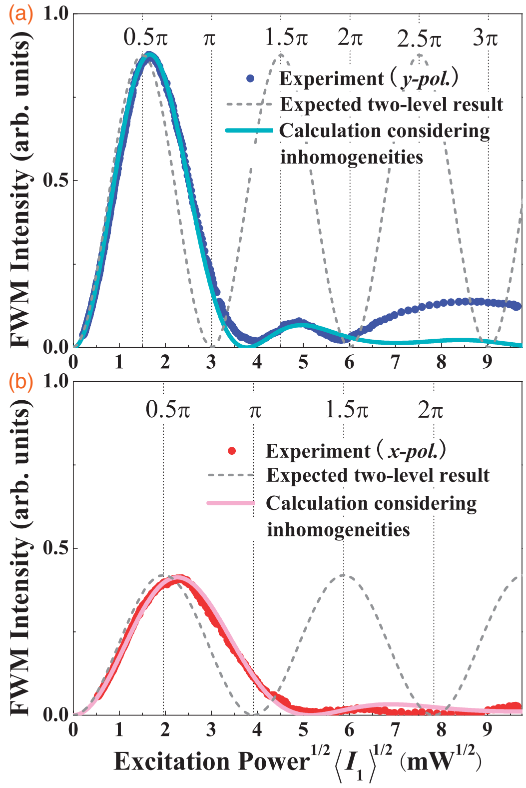

Fig. 1. FWM intensity vs. the average power$^{1/2}$ of the $\boldsymbol{k}_1$ pulse, $\langle I_1\rangle^{1/2}$. The polarization directions of excitation pulses were in (a) $\boldsymbol{y} \parallel [\bar{2}33]$ and (b) $\boldsymbol{x} \parallel [01\bar{1}]$ directions. $\bar{\Theta}_{02}$ was fixed at π. Circles: The experimental results. Lines: The calculated results considering all inhomogeneities (solid lines) and for an ideal two-level system (dashed lines).

The observed signals in Fig. 1, $|\langle S_{\mathrm{FWM}}\rangle|^2$, correspond to the ensemble average of FWM signals generated from a large number of QDs where $E_i(r)$, μ, and Δ are inhomogeneously distributed. We calculate $\langle S_{\mathrm{FWM}}\rangle$ by integrating the FWM signals for the two-level model considering finite detuning with respect to $E_i(r)$, μ, and Δ.[13]

$$\langle S_{\mathrm{FWM}}\rangle \propto \iiint S_{\mathrm{FWM}}(r,\mu,\Delta)f(\mu)g(\Delta)\,dr\,d\mu\,d\Delta,$$

$$S_{\mathrm{FWM}}(r,\mu,\Delta) \propto \frac{\mu\Omega_{01}^*\Omega_{02}^2}{\Omega_1\Omega_2^2}\sin\Theta_1\sin^2\left(\frac{\Theta_2}{2}\right).$$

The generalized Rabi frequency Ω_i is defined as $\Omega_i(E_i,\mu,\Delta) = (\Omega_{0i}^2 + \Delta^2)^{1/2} = \{[\mu E_i(r)/\hbar]^2 + \Delta^2\}^{1/2}$. Also, the generalized pulse area is defined as $\Theta_i(E_i,\mu,\Delta) = \Omega_i(E_i,\mu,\Delta)\pi\tau_{\mathrm{sech}}$ so that Θ_i is equivalent to Θ_{0i} for zero detuning. The quantities $f(\mu)$ and $g(\Delta)$ represent the distribution functions of the number of QDs with μ and Δ, respectively. In the calculation, we used Gaussian distribution functions as follows: $f(\mu) \propto \exp[-(\mu - \bar{\mu})/(2\sigma^2)]$, $g(\Delta) \propto \exp[-\Delta^2/(2\Pi^2)]$. The distribution of the transition dipole moment $\sigma/\bar{\mu} = 0.1$ was estimated from the lateral size distribution of QDs.[16] The inhomogeneous broadening of the detuning Π is assumed to be the same as the spectral width of the excitation pulses, since the contribution of the QDs with large Δ compared to the spectral width is expected to be quite small. Now, we separately discuss the effects of inhomogeneous variations in $E_i(r)$, μ, and Δ on exciton polarization ROs. Figure 2 shows the calculated results taking into account one of the three inhomogeneities at a

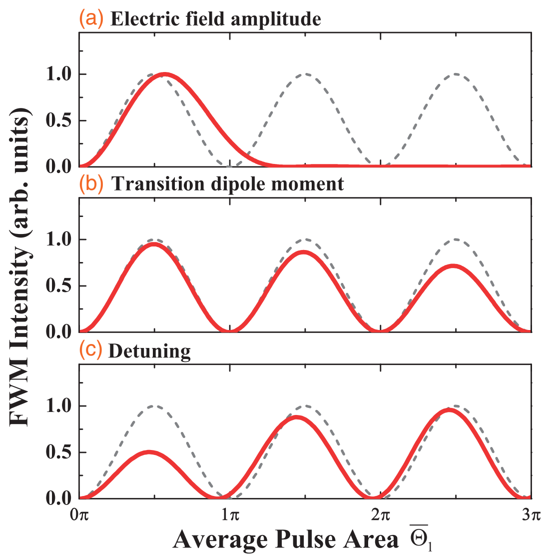

Fig. 2. Effects of the inhomogeneities on macroscopic ROs. Solid lines represent calculated FWM intensities including one of the inhomogeneities; (a) the electric field amplitude, (b) the transition dipole moment, and (c) detuning. Dashed line: calculations for an ideal two-level system $\propto \sin^2 \bar{\Theta}_{01}$.

time. As shown in Figs. 2(a) and 2(b), the inhomogeneities of $E_i(r)$ and μ mainly cause a damping of ROs, while the damping rates are quantitatively different. On the other hand, the integration over Δ induces an increase of the amplitude of macroscopic ROs with increasing pulse area, as shown in Fig. 2(c), since $\Omega_1(E_1, \mu, \Delta)$ approaches Ω_{01} with increasing $\bar{E}_1$.

The solid lines in Fig. 1 show the theoretical curves obtained by the calculation including all inhomogeneities. For $\bar{\Theta}_{01} < 2\pi$, the theoretical curves completely reproduce the experimental results including their anisotropies despite the fact that no fitting parameters apart from the amplitude were used in the calculation. The anisotropies of the excitation intensities $\langle I_1 \rangle^{1/2}$ and the FWM signal intensities at the first peaks are attributed to the anisotropic $\bar{\mu}$ values. The nonharmonic nature of the oscillation period and amplitude are also reproduced by our theoretical calculations for $\bar{\Theta}_{01} < 2\pi$. These nonharmonicities are intrinsic to exciton polarization ROs in a QD ensemble; the FWM signal amplitude is partly compensated in the integration since it may have both positive and negative values. Especially at the minimum point, complete compensation results in a zero value of the ensemble average of the FWM signal intensity. Since the amount of compensation depends on the values of $\bar{\Theta}_{0i}$, the oscillation behavior becomes nonharmonic. This is quite different from exciton population ROs where such compensation cannot occur.

Though we can reproduce most of the experimental results by calculation, we could not explain why the discrepancy between the experiment and calculation becomes apparent at $\Theta > 2\pi$; the signal intensities regained at $\Theta > 2\pi$. This phenomenon is reproducible. This indicates that in large-pulse-area regions, the QD excitons are affected by some nonlinear interactions beyond the two-level approximation. The possible candidates for the origin of this behavior are the local field effect,[9] the biexciton coupling for large pulse areas, and the spatial distribution of the polarization phase. To clarify the origin, further study is necessary.

In summary, we have investigated the exciton polarization ROs in a QD ensemble using an FWM technique. For a small pulse area ($\Theta < 2\pi$), the ensemble-averaged FWM signals in the experiment can be perfectly reproduced, including their anisotropic behaviors, by the calculations considering all inhomogeneities without any fitting parameters. These results strongly confirm that the observed oscillation is in fact originating in ROs due to the QD ensemble. This indicates that our stacked QD sample can indeed be considered as a simple ensemble of isolated two-level systems at least for $\Theta < 2\pi$. The monotonic behavior of the ensemble-averaged FWM signals can be well understood by considering the interference between the exciton polarizations with the inhomogeneously distributed amplitude.

Acknowledgment This work was partly supported by a Grant-in-Aid for Scientific Research from the Ministry of Education, Culture, Sports, Science and Technology.

1) T. H. Stievater, Xiaoqin Li, D. G. Steel, D. Gammon, D. S. Katzer, D. Park, C. Piermarocchi, and L. J. Sham: Phys. Rev. Lett. **87** (2001) 133603.
2) H. Kamada, H. Gotoh, J. Temmyo, T. Takagahara, and H. Ando: Phys. Rev. Lett. **87** (2001) 246401.
3) H. Htoon, T. Takagahara, D. Kulik, O. Baklenov, A. L. Holmes, Jr., and C. K. Shih: Phys. Rev. Lett. **88** (2002) 087401.
4) A. Zrenner, E. Beham, S. Stufler, F. Findels, M. Bichler, and G. Abstreiter: Nature (London) **418** (2002) 612.
5) H. Takagi, T. Nakaoka, K. Watanabe, N. Kumagai, and Y. Arakawa: Opt. Express **16** (2008) 13949.
6) A. Muller, Q. Q. Wang, P. Bianucci, C. K. Shih, and Q. K. Xue: Appl. Phys. Lett. **84** (2004) 981.
7) P. Borri, W. Langbein, S. Schneider, U. Woggon, R. L. Sellin, D. Ouyang, and D. Bimberg: Phys. Rev. B **66** (2002) 081306R.
8) B. Patton, U. Woggon, and W. Langbein: Phys. Rev. Lett. **95** (2005) 266401.
9) Y. Mitsumori, A. Hasegawa, M. Sasaki, H. Maruki, and F. Minami: Phys. Rev. B **71** (2005) 233305.
10) M. Kujiraoka, J. Ishi-Hayase, K. Akahane, Y. Yamamoto, K. Ema, and M. Sasaki: Phys. Status Solidi A **206** (2009) 952.
11) K. Akahane, N. Ohtani, Y. Okada, and M. Kawabe: J. Cryst. Growth **245** (2002) 31.
12) J. Ishi-Hayase, K. Akahane, N. Yamamoto, M. Sasaki, M. Kujiraoka, and K. Ema: Appl. Phys. Lett. **91** (2007) 103111.
13) P. Meystre and M. Sargent: *Elements of Quantum Optics* (Springer, Heidelberg, 1991).
14) M. Kujiraoka, J. Ishi-Hayase, K. Akahane, Y. Yamamoto, K. Ema, and M. Sasaki: J. Lumin. **128** (2008) 972.
15) The pulse area could be considered to be constant in the propagation direction since the optical density for the sample used was quite low and the depth of focus of the excitation pulse was much longer than the total vertical depth of the sample.
16) A. Thränhardt, C. Ell, G. Khitrova, and H. M. Gibbs: Eur. Phys. J. B **27** (2002) 571.